Video Article

Real-Time DC-dynamic Biasing Method for Switching Time Improvement in Severely Underdamped Fringing-field Electrostatic MEMS Actuators

Joshua Small[1], Adam Fruehling[2], Anurag Garg[3], Xiaoguang Liu[1], Dimitrios Peroulis[3]

[1]Department of Electrical and Computer Engineering, University of California, Davis

[2]Digital Light Projection (DLP) Technology Development, Texas Instruments

[3]Birck Nanotechnology Center and the Department of Electrical and Computer Engineering, Purdue University

Correspondence to: Joshua Small at jasmall@ucdavis.edu

URL: http://www.jove.com/video/51251
DOI: doi:10.3791/51251

Keywords: Physics, Issue 90, microelectromechanical systems, actuators, switching time, settling time, electrostatic devices, micromachining, thin film devices

Date Published: 8/15/2014

Citation: Small, J., Fruehling, A., Garg, A., Liu, X., Peroulis, D. Real-Time DC-dynamic Biasing Method for Switching Time Improvement in Severely Underdamped Fringing-field Electrostatic MEMS Actuators. *J. Vis. Exp.* (90), e51251, doi:10.3791/51251 (2014).

Abstract

Mechanically underdamped electrostatic fringing-field MEMS actuators are well known for their fast switching operation in response to a unit step input bias voltage. However, the tradeoff for the improved switching performance is a relatively long settling time to reach each gap height in response to various applied voltages. Transient applied bias waveforms are employed to facilitate reduced switching times for electrostatic fringing-field MEMS actuators with high mechanical quality factors. Removing the underlying substrate of the fringing-field actuator creates the low mechanical damping environment necessary to effectively test the concept. The removal of the underlying substrate also a has substantial improvement on the reliability performance of the device in regards to failure due to stiction. Although DC-dynamic biasing is useful in improving settling time, the required slew rates for typical MEMS devices may place aggressive requirements on the charge pumps for fully-integrated on-chip designs. Additionally, there may be challenges integrating the substrate removal step into the back-end-of-line commercial CMOS processing steps. Experimental validation of fabricated actuators demonstrates an improvement of 50x in switching time when compared to conventional step biasing results. Compared to theoretical calculations, the experimental results are in good agreement.

Video Link

The video component of this article can be found at http://www.jove.com/video/51251/

Introduction

Microelectromechanical systems (MEMS) utilize several actuation mechanisms to achieve mechanical displacement. The most popular are thermal, piezoelectric, magnetostatic, and electrostatic. For short switching time, electrostatic actuation is the most popular technique[1,2]. In practice, critically-damped mechanical designs deliver the best compromise between initial rise time and settling time. Upon applying the DC bias and actuating the membrane down towards the pull-down electrode, the settling time is not a significant issue as the membrane will snap down and adhere to the dielectric coated actuation electrode. Several applications have benefited from the aforementioned electrostatic actuation design[3-8]. However, the presence of the dielectric coated pull-down electrode makes the actuator susceptible to dielectric charging and stiction.

MEMS membranes can utilize an underdamped mechanical design to achieve a fast initial rise time. An example of an underdamped mechanical design is the electrostatic fringing-field actuated (EFFA) MEMS. This topology has exhibited far less vulnerability to typical failure mechanisms that plague electrostatic based designs[9-20]. The absence of the parallel counter electrode and consequently the parallel electric field is why these MEMS are appropriately called “fringing-field” actuated (**Figure 1**). For the EFFA design, the pull-down electrode is split into two separate electrodes that are positioned laterally offset to the moving membrane, completely eliminating the overlap between the movable and stationary parts of the device. However, the removal of the substrate from beneath the movable membrane significantly reduces the squeeze film damping component thereby increasing the settling time. **Figure 2B** is an example of the settling time in response to standard step biasing. Transient, or DC-dynamic applied biasing in real-time can be used to improve the settling time[20-26]. **Figures 2C** and **2D** qualitatively illustrate how a time varying waveform can effectively cancel the ringing. Previous research efforts utilize numerical methods to calculate the precise voltage and timings of the input bias to improve the switching time. The method in this work uses compact closed form expressions to calculate the input bias waveform parameters. Additionally, previous work focused on parallel plate actuation. While the structures are designed to be underdamped, squeeze-film damping is still available in this configuration. The actuation method presented in this work is fringing-field actuation. In this configuration squeeze-film damping is effectively eliminated. This represents an extreme case where the mechanical damping of the MEMS beam is very low. This paper describes how to fabricate the EFFA MEMS devices and perform the measurement to experimentally validate the waveform concept.

Protocol

1. Fabrication of EFFA MEMS Fixed-fixed Beams (See Figure 3 for Summarized Process)

1. UV lithography and chemical wet etch of silicon dioxide with buffered hydrofluoric acid (CAUTION[27]).
    1. Use an oxidized, low resistivity silicon substrate.
    2. Fill a glass beaker with acetone[28] (enough to submerge the sample), place the sample in the acetone filled beaker, and sonicate for 5 min in a water bath sonicator.
    3. Without drying, directly transfer the sample from the acetone beaker to a beaker filled with isopropyl alcohol[29] and sonicate for 5 min in a water-bath sonicator.
    4. Dry the sample with nitrogen (do not allow the isopropyl alcohol to evaporate from the surface).
    5. Dry (dehydration bake) the sample on a hotplate set to 150 °C for 10 min. Allow the sample to reach RT once the dehydration bake is complete.
    6. Place the sample on the chuck of a photoresist spinner. Pipette and dispense 1 ml of hexamethyldisilazane (HMDS) per 25 mm of diameter (CAUTION[30]). Spincoat at 3,500 rpm for 30 sec. Pipette and dispense 1 ml of positive photoresist per 25 mm of diameter (CAUTION[31]). Spincoat the sample at 3,500 rpm for 30 sec. Softbake the photoresist for 90 sec at 105 °C on a hotplate.
    7. Use a mask aligner to expose the sample to UV radiation with a wavelength of 350-450 nm. Use exposure energy of 391 mJ/cm^2 (CAUTION[32]).
    8. Fill a glass beaker with TMAH based developer (CAUTION[33]) and use enough to submerge the entire sample.
    9. Fill a glass beaker with deionized water to quickly terminate the development to avoid overdevelopment.
    10. Develop the sample for 12-20 sec. Gently agitate the submerged sample.
    11. Carefully and quickly remove the sample from the development beaker and submerge it in the rinse water beaker for 10 sec.
    12. Rinse the sample in a sink under running deionized water for 1-2 min.
    13. Carefully blow dry the sample with nitrogen (Do not allow the deionized water to evaporate from the surface).
    14. Inspect the sample under a microscope.
    15. If necessary, repeat the development procedure with adjustments in time to avoid overdevelopment.
    16. Use a plasma reactive ion etch (RIE) to roughen the surface to improve the surface wetting. RIE settings[34]: 100 sccm of Ar, 100 W RF power, 50 mT chamber pressure, 1 min.
    17. Fill a Teflon beaker with a sufficient amount of buffered oxide etch (BOE) to cover the sample.
    18. Fill another Teflon beaker with deionized water for an intermediate rinse of the sample.
    19. Submerge the sample in the BOE. The etch rate is 90-100 nm/min.
    20. When the etch is complete, rinse in the Teflon beaker that has deionized water for 10 sec. Then rinse the sample in a sink under running deionized water for 1-2 min.
    21. Dry the sample with nitrogen (Do not allow the deionized water to evaporate from the surface).
    22. Inspect the sample under a microscope.
    23. Repeat the etch and rinse steps as necessary with adjustments in the time in order to avoid over-etching and undercutting of the photoresist.
    24. Remove photoresist mask.
    25. Fill a glass beaker with acetone (enough to submerge the sample), place the sample in the acetone filled beaker and sonicate in a water-bath sonicator for 5 min.
    26. Directly take the sample from the acetone beaker and place it in an isopropyl alcohol filled beaker and sonicate for 5 min in a water-bath sonicator.
    27. Dry the sample with nitrogen (Do not allow the isopropyl alcohol to evaporate from the surface).
2. Chemical wet etch of silicon with tetramethylammonium hydroxide (TMAH) 25% by weight (CAUTION[35]).
    1. Use a clean 4 L beaker.
    2. Use a hotplate with a thermocouple. Use a Teflon basket that has a hook at the end of the handle for holding the samples. Use a magnetic stir rod for proper agitation to alleviate the silicon surface of hydrogen bubbles that are released during the bulk etching process.
       NOTE: The feedback between the thermocouple and the hotplate ensures the appropriate temperature remains constant throughout the etch. If the released hydrogen is not removed from the surface, it may mask the underlying silicon from the TMAH.
    3. Pour the TMAH 25% by weight up to the 2 L mark of the beaker.
    4. Place the thermocouple in the solution and preheat to 80 °C. If possible, use a custom fixture or clamp to hold the thermocouple to prevent interference with the rotation of the magnetic stir bar.
    5. Once the solution reaches the necessary temperature, place the samples in the Teflon basket and place the basket in the solution by hanging it from the lip of the beaker. Make sure that the basket does not rest on the bottom of the beaker in order to leave room for the magnetic stir rod to rotate.
    6. Set the rotation rate of the magnetic stir bar to 400 rpm.
    7. The etch rate of the solution is 300-350 nm/min. The necessary etch depth is 4-5 µm.
    8. When the necessary time has elapsed to complete the etch, remove the sample from the solution and rinse with deionized water for 1-2 min.
    9. Dry the sample with nitrogen (Do not allow the deionized water to evaporate from the surface).
    10. Use a profilometer to measure the step height.
    11. If the step height has not been reached, place the samples in the solution again in order to achieve the desired step height.
3. Chemical wet etch of all SiO_2 from the substrate and thermally grow another 500 nm of SiO_2.
    1. Fill a Teflon beaker with hydrofluoric acid 49% by volume (CAUTION[36]). Use an amount that is sufficient to cover the sample.

2. Fill a Teflon beaker with deionized water for rinsing the sample. Use an amount that is sufficient to cover the sample.
3. Etch the sample with hydrofluoric acid. Leave the sample in the solution until all of the SiO_2 is removed. Since the solution is highly concentrated, the etch will occur relatively quickly.
4. Rinse for 10-20 sec in the Teflon beaker filled with deionized water.
5. Rinse the sample thoroughly under running deionized water in a sink for 1-2 min.
6. Mix a solution of H_2SO_4:H_2O_2 (sulfuric acid:hydrogen peroxide, piranha clean) in a 1:1 ratio in a Teflon beaker (CAUTION[37]). Use enough to cover the sample.
7. Fill a Teflon beaker with deionized water for rinsing the sample.
8. Submerge the sample in the H_2SO_4:H_2O_2 for 7-10 min.
9. Briefly, 10 sec, rinse the sample in the rinse water beaker.
10. Thoroughly rinse the sample in a sink under running deionized water for 1-2 min.
11. Dry the sample with nitrogen (Do not allow the water to evaporate from the surface).
12. Perform wet thermal oxidation to grow 500 nm of SiO_2.

4. UV lithography and chemical wet etch to pattern the SiO_2 to expose the silicon which serves as the sacrificial layer for the final release of the fixed-fixed beams.
    1. Fill a glass beaker with acetone (enough to submerge the sample), place the sample in the acetone filled beaker and sonicate in a water-bath sonicator for 5 min.
    2. Directly take the sample from the acetone beaker and place it in an isopropyl alcohol filled beaker and sonicate in a water-bath sonicator for 5 min.
    3. Dry the sample with nitrogen (Do not allow the isopropyl alcohol to evaporate from the surface).
    4. Dry (dehydration bake) the sample on a hotplate set to 150 °C for 10 min. Allow the sample to reach RT once the dehydration bake is complete.
    5. Using a photoresist spincoater, spincoat HMDS on the sample at 3,500 rpm for 30 sec. Using a photoresist spincoater, spincoat positive photoresist on to the sample at 3,500 rpm for 30 sec. Softbake the photoresist for 90 sec at 105 °C on a hotplate.
    NOTE: Use 1 ml per every 25 mm of sample diameter.
    6. Use a mask aligner to expose the sample to UV radiation with a wavelength of 350-450 nm. Use exposure energy of 391 mJ/cm^2.
    7. Fill a glass beaker with a TMAH based developer and use enough to submerge the entire sample.
    8. Fill a glass beaker with deionized water to quickly terminate the development to prevent overdevelopment.
    9. Develop the sample for 12-20 sec.
    10. Carefully and quickly remove the sample from the development beaker and submerge it in the rinse water beaker for 10 sec.
    11. Rinse the sample in a sink under running deionized water for 1-2 min.
    12. Carefully dry with nitrogen (Do not allow the water to evaporate from the surface).
    13. Inspect the sample under a microscope.
    14. If necessary, repeat the development procedure with adjustments in time to avoid overdevelopment.
    15. Use plasma RIE to roughen the surface to improve the surface wetting. RIE settings: 100 sccm of Ar, 100 W RF power, 50 mT chamber pressure, 1 min.
    16. Fill a Teflon beaker with a sufficient amount of BOE to cover the sample.
    17. Fill a Teflon beaker with deionized water for an intermediate rinse of the sample.
    18. Submerge the sample in the BOE. The etch rate is 90-100 nm/min.
    19. When the etch is complete, rinse in the Teflon beaker that has deionized water for 10 sec. Then rinse the sample under running deionized water in a sink for 1-2 min.
    20. Dry the sample with nitrogen (Do not allow the water to evaporate from the surface).
    21. Inspect sample under a microscope.
    22. Repeat the etch and rinse steps as necessary with adjustments in the time in order to avoid over-etching and undercutting of the photoresist.
    23. Fill a glass beaker with acetone (enough to submerge the sample), place the sample in the acetone filled beaker, and sonicate in a water-bath sonicator for 5 min.
    24. Directly take the sample from the acetone beaker and place it in an isopropyl alcohol filled beaker and sonicate in a water-bath sonicator for 5 min.
    25. Dry the sample with nitrogen (Do not allow the isopropyl alcohol to evaporate from the surface).

5. Sputter deposit 20 nm of Ti and 100 nm of Au. This film serves as the electroplating seed layer for the subsequent electroplating process step. The sputtering parameters are: DC power of 100 W, deposition pressure of 8 mT, 100 sccm of Ar, base pressure 3 x 10^{-6} T.
    1. Vent the process chamber or load lock to atmosphere.
    2. Load the sample into the process chamber or load lock.
    3. Pump the process chamber or load lock to vacuum.
    4. Wait until the process chamber achieves a base pressure of 3 x 10^{-6} T.
    5. Position the sample to the appropriate place for deposition.
    6. Set the chamber pressure to 8 mT by flowing argon into the system. The exact flow rate needed to achieve 8 mT highly dependent on the type of system used. The sputtering tool used for this work used a flow rate of 100 sccm.
    7. Activate the source with the titanium target.
    8. Presputter titanium at 300 W for 20 min.
    9. Sputter 20 nm of titanium at 100 W. The exact time of the deposition is highly dependent on the type of system use. For the sputtering tool used in this work, 5 min is necessary to achieve 20 nm.
    10. Deactivate the source with the titanium sputtering target.
    11. Activate the source with the gold target.
    12. Presputter gold at 100 W for 2 min.
    13. Sputter 100 nm of gold at 100 W. The exact deposition time is highly dependent on the sputtering tool that is used. For the sputtering tool used in this work, 10 min is enough to provide 100 nm of gold.

14. Deactivate the source with the gold sputtering target.
15. Close the Ar gas valve.
16. Vent the process chamber or load lock.
17. Unload the sample once the process chamber or load lock reaches atmosphere.
18. Pump the load lock or process chamber down to high vacuum.

6. UV lithography to create a photoresist mold that defines the geometry of the fixed-fixed beam.
    1. Fill a glass beaker with acetone (enough to submerge the sample), place the sample in the acetone filled beaker for 5 min.
    2. Directly take the sample from the acetone beaker and place it in an isopropyl alcohol filled beaker for 5 min.
    3. Dry the sample with nitrogen (Do not allow the isopropyl alcohol to evaporate from the surface).
    4. Dry (dehydration bake) the sample on a hotplate set to 150 °C for 10 min. Allow the sample to reach RT once the dehydration bake is complete.
    5. Using a photoresist spincoater, spincoat HMDS on the sample at 3,500 rpm for 30 sec. Using a photoresist spincoater, spincoat positive photoresist on to the sample at 2,000 rpm for 30 sec. Softbake the photoresist for 90 sec at 105 °C on a hotplate.
    NOTE: Use 1 ml per every 25 mm of sample diameter.
    6. Use a mask aligner to align and expose the sample to UV radiation with a wavelength of 350-450 nm. Use an exposure energy of 483 mJ/cm^2.
    7. Fill a glass beaker with TMAH based developer and use enough to submerge the entire sample.
    8. Fill a glass beaker with deionized water to quickly terminate the development in order to prevent overdevelopment.
    9. Develop the sample for 12-20 sec.
    10. Carefully and quickly remove the sample from the development beaker and submerge it in the rinse water beaker for 10 sec.
    11. Rinse the sample in a sink under running deionized water for 1-2 min.
    12. Dry the sample with nitrogen (Do not allow the water to evaporate from the surface).
    13. Inspect the sample under a microscope.
    14. If necessary, repeat the development procedure with adjustments in time to avoid overdevelopment.

7. Electroplate gold MEMS beam.
    1. Use a 1 L beaker glass beaker.
    2. Fill beaker with 700 ml of a commercially-available, ready-to-use gold electroplating solution (CAUTION[38]).Place filled beaker on a hotplate.
    3. Set the hotplate to 60 °C. Use a thermocouple to ensure that the solution stays at the desired temperature. Once the solution has reached the desired temperature, attach the sample to a fixture that holds the anode, workpiece (the sample), and the thermocouple.
    4. Set the current supply to the appropriate amplitude based on the exposed metalized area of the sample. A constant current density of 2 mA/cm^2 is used.
    5. A stainless steel anode is used.
    6. Connect the live to the anode and the ground to the sample.
    7. The deposition rate is 250-300 nm/min. The final thickness of the fixed-fixed beam is 0.5 µm. Taking into consideration that an approximate 4:1 ratio exists in the etch rates of electroplated to sputtered gold (when removing the sputtered seed layer), the beam is electroplated to 1 µm.
    8. When the necessary time has elapsed, turn off the current supply, disconnect the leads from the anode and workpiece, remove the sample, and rinse thoroughly under running deionized water in a sink for 1 min.
    9. Blow dry the sample with nitrogen (Do not allow the water to evaporate from the surface).
    10. Use a microscope and profilometer to verify that the electroplating is complete.

8. Etch the photoresist mold.
    1. Preheat glass beaker filled with a dedicated photoresist stripper on a hotplate to 110 °C (CAUTION[39]). Submerge sample in the solution for 1 hr.
    2. Remove the beaker from hotplate and allow the solution and sample to reach RT.
    3. Rinse sample thoroughly under running water in a sink for 1-2 min.
    4. Submerge sample in a beaker filled with acetone for 5 min.
    5. Submerge sample in a beaker filled with isopropyl alcohol for 5 min.
    6. Dry the sample with nitrogen (Do not allow the isopropyl alcohol to evaporate from the surface).
    7. Inspect sample under a microscope and measure the step height of the electroplated Au with a profilometer. Repeat the cleaning steps if necessary.

9. Chemical wet etch Ti/Au seed layer.
    1. Place sample in plasma RIE and use the following parameters: 100 sccm of Ar, 100 W, 50 mT for 30 sec.
    2. Fill a Teflon or glass beaker with Au etchant (CAUTION[40]). Use enough to cover the entire sample.
    3. Fill a Teflon or glass beaker with deionized water. This beaker will serve as an intermediate rinse beaker to quickly terminate the Au etch.
    4. Submerge the sample in the Au etchant. Etch parameters - RT, 7-8 nm/sec, agitated. Once etch is complete, submerge the sample in the rinse water beaker and gently agitate for 10-20 sec.
    5. Rinse the sample thoroughly under running deionized water in a sink for 1-2 min.
    6. Nitrogen blow dry (Do not allow the water to evaporate from the surface).
    7. Inspect the etch under a microscope and, if necessary, repeat until all the Au is removed from the exposed areas.
    8. Perform plasma RIE again on the sample with the following parameters: 100 sccm of Ar, 100 W, 50 mT for 30 sec.
    9. Fill a Teflon beaker with BOE (enough to submerge the sample).
    10. Fill a Teflon with deionized water for rinsing the sample.
    11. Submerge the sample in the BOE at RT. The etch rate is 15-18 nm/min.When the etch time is complete, remove the sample from the beaker and submerge it into the rinse beaker for 10-20 sec.

12. Rinse the sample thoroughly under running deionized water in a sink for 1-2 min.
13. Nitrogen blow dry (Do not allow the water to evaporate from the surface).
14. Inspect etch and, if necessary, repeat until all the titanium is removed from the exposed areas. Reduce the etch time to avoid significant undercutting.

10. Perform a dry isotropic XeF_2 etch (CAUTION[41]) that selectively removes the silicon and releases the Au fixed-fixed beams.
    1. Vent the process chamber to atmosphere.
    2. Load the sample in the process chamber.
    3. Pump the system down to vacuum.
    4. The etch time strongly depends on the exposed area and the type of etch system used. For this sample a pressure of 3 T with a 30 sec cycle is used. 10 cycles are used. An etch rate of 110-120 nm/min is extracted.
    5. Once the etch parameter are set in the system, etch the silicon sacrificial layer.
    6. When the etch is complete perform the necessary purging steps to ensure toxic gases are removed before venting the system to atmosphere. The system in this study has a process that automatically performs this purge step.
    7. Vent the process chamber to atmosphere.
    8. Carefully remove the samples.
    9. Pump the process chamber down to vacuum.

2. Experimental Validation of Dynamic Waveform

1. Load sample on DC probe station.
    1. Place the sample on the chuck of the DC probe station.
    2. Activate the vacuum of the chuck to hold the sample down.
    3. Use DC probe tip manipulators to position the tungsten probe tips on the biasing pads of the MEMS bridges.
    4. Use the microscope of the DC probe station to view the precise positioning of the tungsten probe tips over the DC biasing pads of the device. The fixed-fixed beam is probed with the live signal probe tip while the pull down electrodes are probed with the ground probe tip.

2. Program dynamic biasing signal on the function generator.
    1. Use calculated values for the initial wave parameters[20].
    2. Choose the arbitrary waveform function on the function generator to create the dynamic waveform.
    3. Input the time parameters of the waveform. Depending on the type of function generator, the first time parameter starts after few microseconds (as opposed to 0 µsec). The interval between the first and second time parameter will be the calculated time it will take the beam to reach the overshoot gap. The interval between the second and third time parameter should be long enough to allow the beam to completely reach equilibrium with minimal oscillation. When inputting the time parameters to operate in the reverse direction (from pull-down to release), the overshoot gap time will determine the time interval between the third time parameter and turning off the. There will be a fifth time interval need to restart the wave. For this interval permit sufficient time for the beam to reach equilibrium before restarting the cycle.
    4. Input the voltage parameters of the waveform. The voltages will be a fraction of the actual voltage applied to the beam because this signal will pass through a linear amplifier. The values programmed into the function generator for this study were 1/20 of the actual voltage.
    5. Connect the output of the function generator to the high-speed high-voltage linear amplifier.
    6. Connect the output of the linear amplifier to a digital oscilloscope with sampling rate of 300 MHz. The oscilloscope is used to verify the signal output from the arbitrary waveform generator.
    7. Connect the output of the linear amplifier to the DC manipulators. Make sure the function generator is off while performing this step.

3. Setup and measure with the Laser Doppler vibrometer (LDV)
    1. Position the head that holds the LDV over the sample.
    2. Turn on the laser.
    3. Use the microscope that is integrated with the LDV to find the desired beam to measure.
    4. Focus the laser on the center of the MEMS bridge. This is the point of maximum deflection.
    5. Ensure the intensity of the laser beam reflection is sufficient for accurate measurement.
    6. Set the sampling time to the appropriate sampling rate. This measurement uses a sampling rate of 5.1 MHz.
    7. Select the displacement versus time output for the LDV.
    8. Select the continuous measurement mode.
    9. Apply the biasing signal on the MEMS bridges. The LDV will capture the ringing effect in real-time.
    10. Tune the timing and voltage parameters on the function generator to achieve minimal beam oscillation on the pull-down and release operations.
    11. Once the optimal values are found turn off the biasing signal.
    12. Turn off the continuous LDV measurement mode.
    13. Lift the DC probe tips up from the biasing pads.
    14. Connect the triggering input of the function generator to the triggering output of the LDV hardware interface. For this study a BNC cable is used for this connection.
    15. Set the function generator to acknowledge the external trigger from the LDV system.
    16. Set the LDV software to trigger the function generator when the measurement scan mode begins.
    17. Set the LDV software to single scan mode. The time single scan will be the duration of the waveform.
    18. Drop the DC probe tips back down on the biasing pads of the MEMS bridge.
    19. Capture the signal scan by activating the measurement mode of the LDV.

20. Save the displacement versus time data.

Representative Results

The setup in **Figure 4** is used to capture the deflection versus time characteristics of the MEMS bridges. By using the laser doppler vibrometer in its continuous measurement mode, the precise voltage and time parameters can be found to result in minimum beam oscillation for the desired gap height. **Figure 5** illustrates an example beam deflection corresponding to the 60 V gap height. It is seen that virtually all of the oscillation is removed. Not only is the dynamic waveform useful for one gap height, but for all of the gap possible heights. This is demonstrated in **Figure 6** and **Figure 7** for both the pull-down and release operations, respectively. The calculated and measured dynamic wave form used to achieve the measurements in the previous figures is presented in **Figures 8** and **9**, respectively.

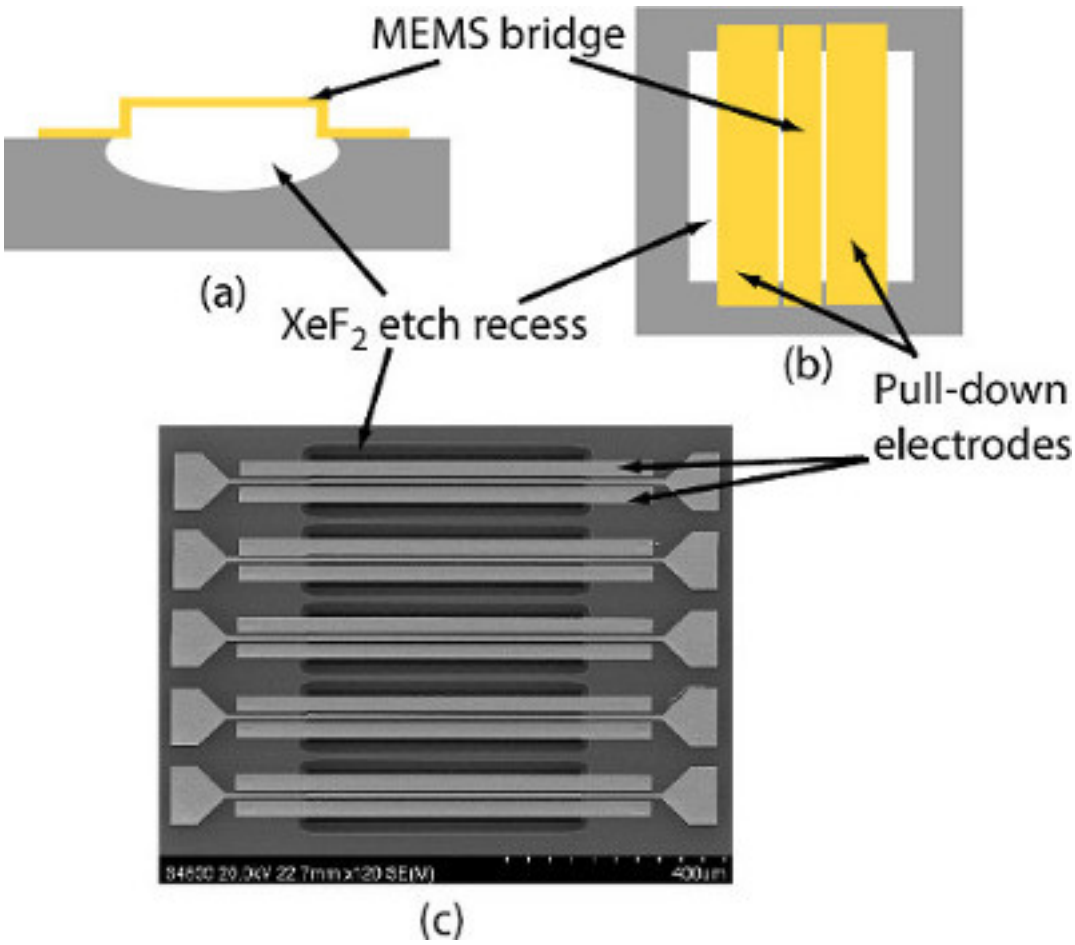

Figure 1. 2D sketch and SEM image of MEMS bridges used in this study. (A) 2D profile. **(B)** Top view of MEMS bridges. **(C)** SEM of actual fabricated device. Please click here to view a larger version of this figure.

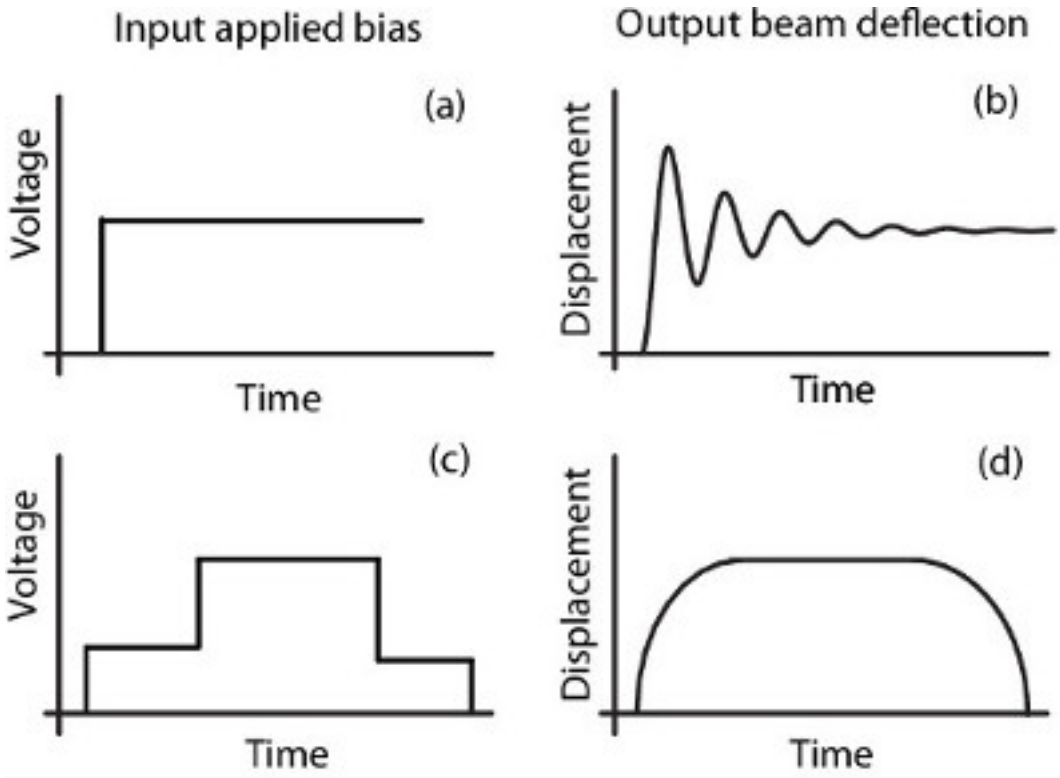

Figure 2. Sketch of underdamped MEMS bridge in response to an input step and time varying response. (A) Unit step applied bias. **(B)** Response of underdamped MEMS bridge to unit step input. **(C)** Time varying/dynamic input bias. **(D)** Response of MEMS bridge to time varying input. Please click here to view a larger version of this figure.

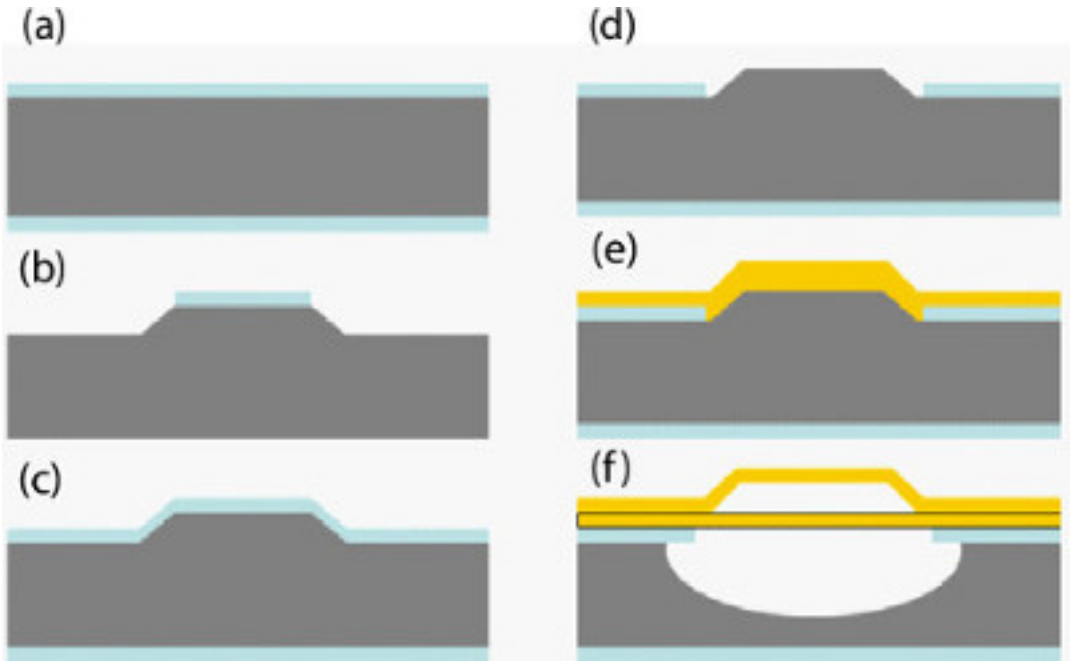

Figure 3. Summarized process flow for the MEMS bridges. (A) Oxidized silicon substrate. **(B)** Bulk etch of silicon substrate. **(C)** Re-oxidation of silicon substrate. **(D)** Silicon dioxide etch to expose sacrificial silicon. **(E)** Gold deposition and patterning. **(F)** Etch of sacrificial silicon layer to release the MEMS bridge. Please click here to view a larger version of this figure.

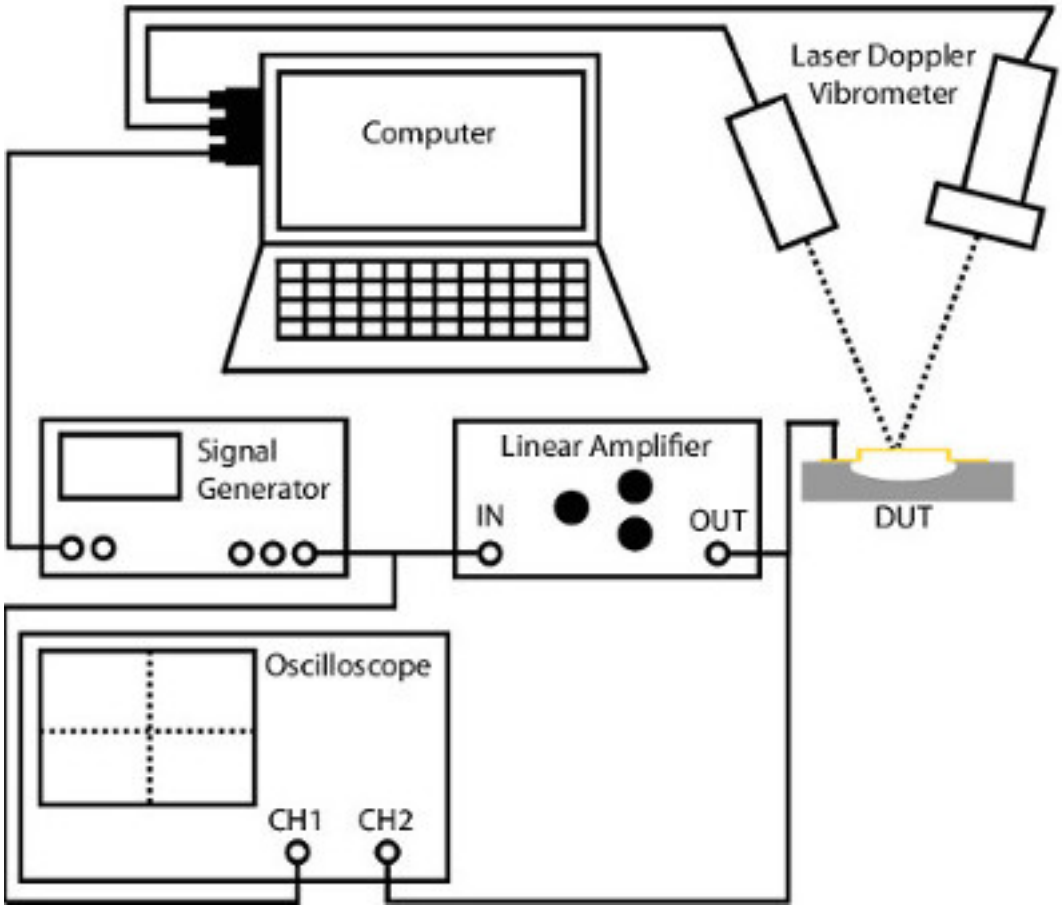

Figure 4. Block diagram of the experimental setup used to apply the bias signal and capture the MEMS bridge deflection. Please click here to view a larger version of this figure.

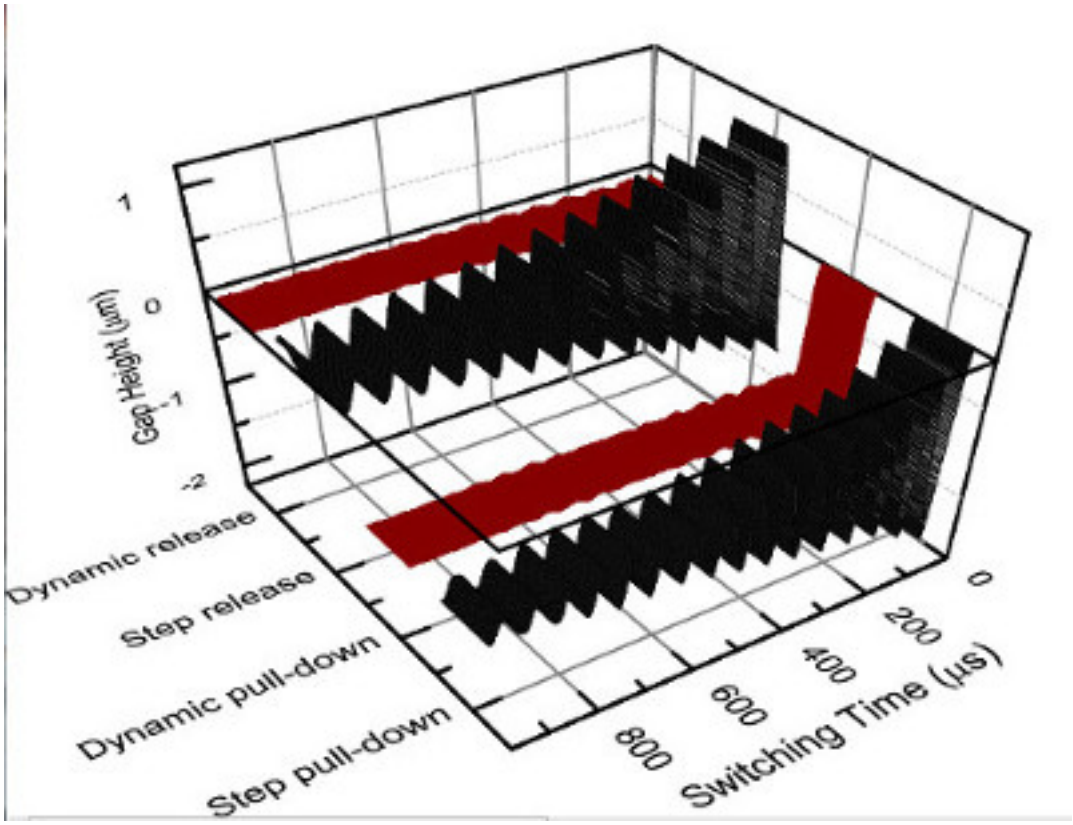

Figure 5. Measured pull-down and release states of a MEMS bridge in response to a 60 V input bias. The black curve is the response from a step input. The red curve is the response to a dynamic input.

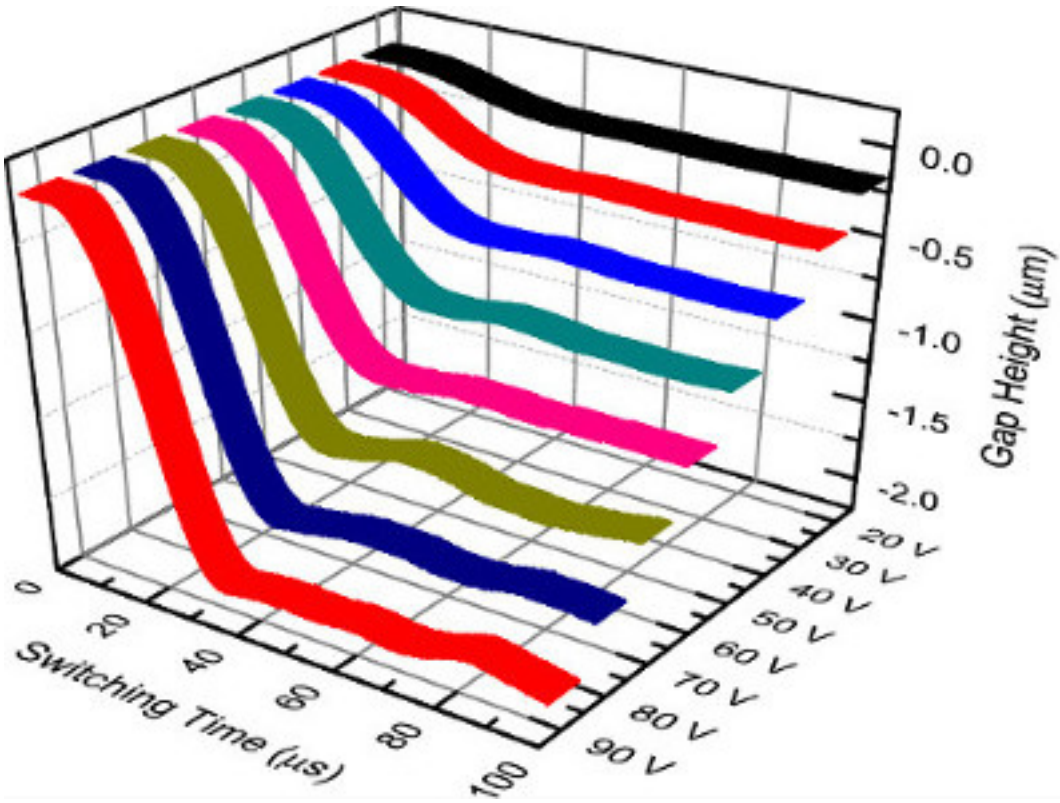

Figure 6. Measured intermediate pull-down gap heights of the MEMS bridge in response to a dynamic input. Please click here to view a larger version of this figure.

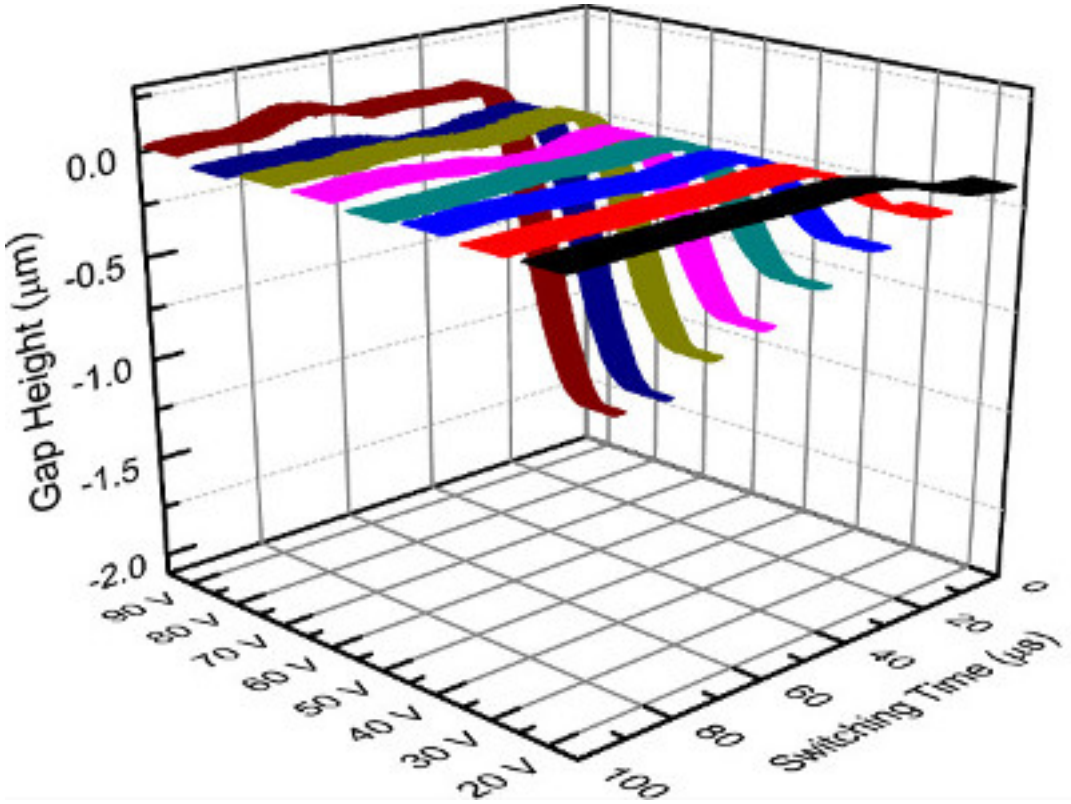

Figure 7. Measured intermediate release gap heights of the MEMS bridge in response to a dynamic input.

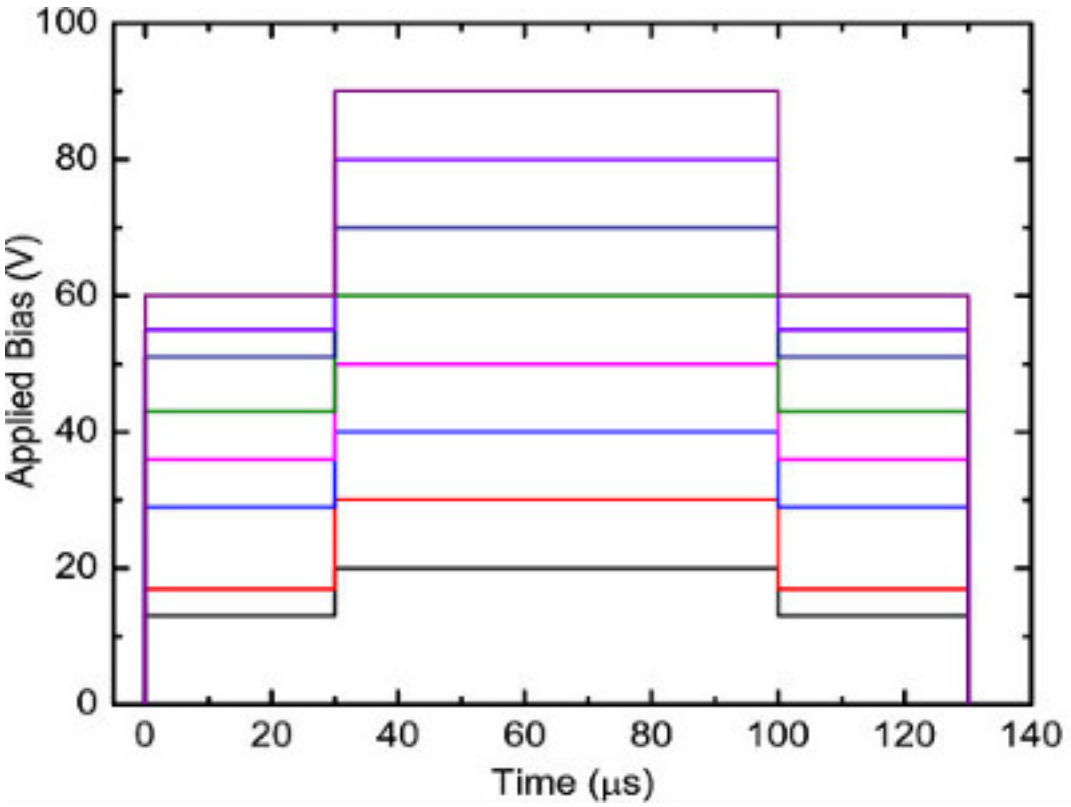

Figure 8. Calculated waveform for the input bias.

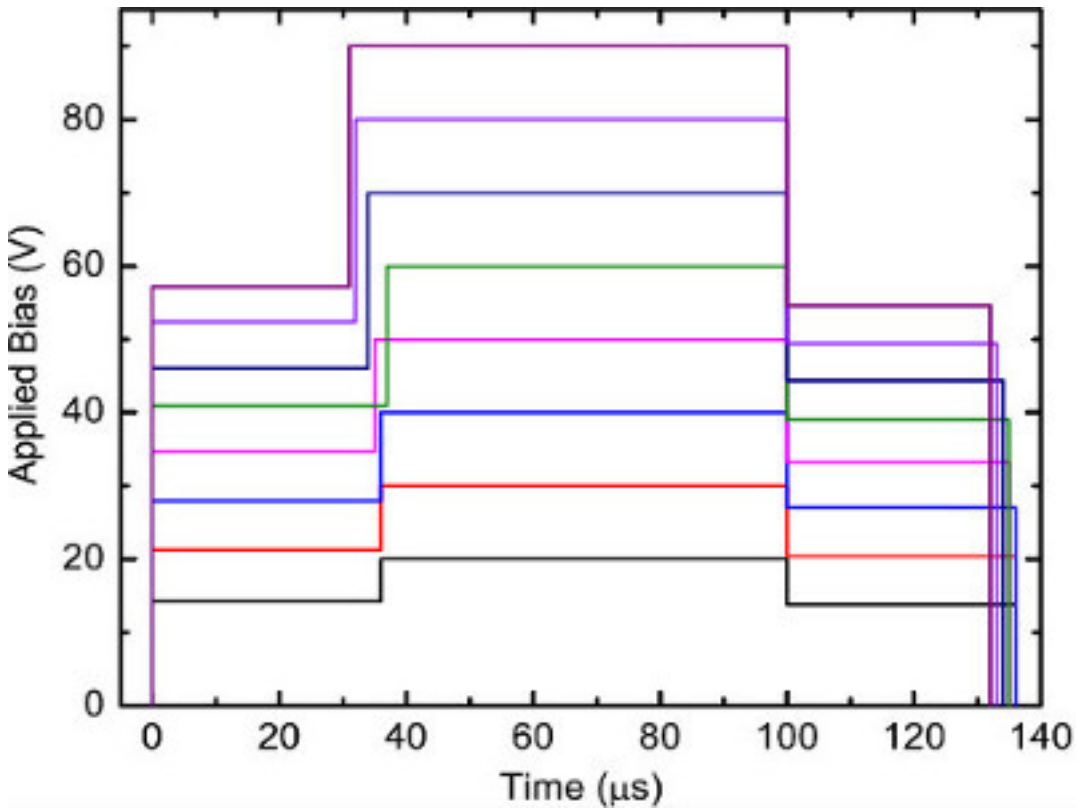

Figure 9. Actual waveform used to achieve minimum oscillation of the MEMS bridge.

Discussion

Low residual stress Au film deposition and a dry release with XeF_2 are critically components in the successful fabrication of the device. Electrostatic fringing-field actuators provide relatively low forces when compared to parallel-plate field actuators. Typical MEMS thin film stresses of >60 MPa will result in excessively high drive voltages which can potentially compromise the reliability of EFFA MEMS. For this reason the electroplating recipe is carefully characterized to yield a thin film with low bi-axial mean stress. Additionally, this study uses silicon as the sacrificial layer type due to its relative lack of expansion and contraction (compared to photoresist) during process steps that require heat cycles. Finally, the dry release step with XeF_2 facilitates high yield processing by virtually eliminating stiction.

The desired beam gap height corresponds to the overshoot gap height (**Figure 2B**) in response to the first step bias[20]. Once the beam attains the overshoot/desired gap height the second step bias (**Figure 2C**) is applied to hold the beam in this position. By knowing the mechanical quality factor of the MEMS bridge (which can be measured or calculated), the overshoot percentage and the time to reach the overshoot gap height can be calculated. These parameters are used to determine the amplitude and timing of the input voltage.

DC-dynamic drive signals used in this study improved the settling time from ~2 msec down to ~35 µsec for both up-to-down and down-to-up states. The calculated switching time using the heuristic model[20] is 28 µsec for a beam with width w = 10 µm, length L = 400 µm, thickness t = 0.45 µm, lateral pull-down gap s = 8 µm, and residual tensile mean stress σ = 5 MPa. Switching time has a $\sigma^{-1/2}$ relationship[20]. The consequence of this relationship is that relatively small variations in the residual stress can have a non-marginal impact on the switching time calculation. A relatively small difference of 2 MPa in residual stress can result in a switching time variation of 20%. Therefore a need exists for real-time optimization with the method presented in this paper due to the inevitability of process variation across a wafer.

The method presented in this work demonstrates significant improvements in switching time for electrostatic fringing field actuators where the substrate is removed. The details for fabrication of the EFFA MEMS tuners and the electrical testing are described in detail. The experimental method, in particular the dynamic biasing technique, will find utility in virtually any mechanically underdamped MEMS design in regards to improving the switching time performance.

Disclosures

The authors have nothing to disclose.

Acknowledgements

The authors wish to thank Ryan Tung for his assistance and useful technical discussions.

The authors also wish to acknowledge the assistance and support of the Birck Nanotechnology Center technical staff. This work was supported by the Defense Advanced Research Projects Agency under the Purdue Microwave Reconfigurable Evanescent-Mode Cavity Filters Study. And also by NNSA Center of Prediction of Reliability, Integrity and Survivability of Microsystems and Department of Energy under Award Number DE-FC5208NA28617. The views, opinions, and/or findings contained in this paper/presentation are those of the authors/presenters and should not be interpreted as representing the official views or policies, either expressed or implied, of the Defense Advanced Research Projects Agency or the Department of Defense.

References

1. Rebeiz, G. RF MEMS: Theory, Design, and Technology. *John Wiley and Sons.* (2003).
2. Senturia, S. D. Microsystem Design. *Springer.* (2001).
3. Bouchaud, J. Propelled by HP Inkjet Sales, STMicroelectronics Remains Top MEMS Foundry. *http://www.isuppli.com/MEMS-and-Sensors/News/Pages/Propelled-by-HP-Inkjet-Sales-STMicroelectronics-Remains-Top-MEMS-Foundry.aspx.* (2011).
4. Lantowski, K. G. D. The Future of Cinema Has Arrived: More Than 50,000 Theatre Screens Worldwide Feature The Brightest, 2D/3D Digital Cinema Experience With DLP Cinema. *http://www.dlp.com/technology/dlp-press-releases/press-release.aspx?id=1510.* (2011).
5. Bosch-Wachtel, T. Knowles Ships 2 Billionth SiSonic MEMS Microphone. *http://pressrelease.smartoman.com/?p=2810.* (2011).
6. Burke, J. Mirasol Display Capabilities Add Color and Interactivity to Improve User Experience for Renowned Jin Yong Branded Device *http://www.mirasoldisplays.com/press-center/pressreleases/2012/01/koobe-taiwan%E2%80%99s-leading-e-reader-manufacturer-and-qualcommbring.* (2012).
7. Bettler, D. *MEMStronics Captures Prestigious R & D 100 Award.* http://www.memtronics.com/files/MEMtronics_Press_Release7_1_2011.pdf. (2011).
8. Marsh, C. Omron Releases New RF MEMS Switch with Superior High Frequency Characteristics rated to 100 Million Operations *http://www.components.omron.com/components/web/pdflib.nsf/0/. D69D5B6BCBE68DC2862574FD005B5141/$file/Omron 2MES-1 PR final.pdf.* (2008).
9. Rosa, M. A., Bruyker, D. D., Volkel, A. R., Peeters, E., & Dunec, J. A novel external electrode configuration for the electrostatic actuation of MEMS based devices. *J. Micromech. Microeng.* **14.** 446-451 (2004).
10. Rottenberg, X. *et al.* Electrostatic fringing-field actuator (EFFA): application towards a low-complexity thin film RF-MEMS technology. *J. Micromech. Microeng.* **17**, S204-S210 (2007).
11. Allen, W. N., Small, J., Liu, X., & Peroulis, D. Bandwidth-optimal single shunt-capacitor matching networks for parallel RC loads of Q >> 1. *Asia-Pacific Microw. Conf. (Singapore).* 128-2131 (2009).
12. Small, J., Liu, X., Garg, A., & Peroulis, D. Electrostatically tunable analog single crystal silicon fringing-field MEMS varactors. *Asia-Pacific Microw. Conf. (Singapore).* 75-578 (2009).
13. Liu, X., Small, J., Berdy, D., Katehi, L. P. B., Chappell, W. J., & Peroulis, D. Impact of mechanical vibration on the performance of RF MEMS evanescent-mode tunable resonators. *IEEE Microw. Wireless Compon. Lett.* **21,** 406-408 (2011).
14. Small, J., *et al.* Electrostatic fringing field actuation for pull-in free RF-MEMS analog tunable resonators. *J. Micromech. Microeng.* **22**, 095004 , (2012).
15. Su, J. A lateral-drive method to address pull-in failure in MEMS. *Ph.D. Dissertation Dept. Elect. Comput. Eng., University of Notre Dame.*(2008).
16. Scott, S., & Peroulis, D. A capacitively-loaded MEMS slot element for wireless temperature sensing of up to 300 °C. *IEEE MTT-S Int. Microwave Symp. Dig. (Boston, MA, USA).* 161-1164 (2009).
17. Scott, S., Sadeghi, F., & Peroulis, D. Inherently-robust 300C MEMS sensor for wireless health monitoring of ball and rolling element bearings. *IEEE Sensors (Christchurch, New Zealand).* 75-978 (2009).
18. Lee, K. B. Non-contact electrostatic microactuator using slit structures: theory and a preliminary test. *J. Micromech. Microeng.* **17**, 2186-96 (2007).
19. Su, J., Yang, H., Fay, P., Porod, W., & Berstein, G. H. A surface micromachined offset-drive method to extend the electrostatic travel range. *J. Micromech. Microeng.* **20**, 015004 (2010).
20. Small, J., A. Fruehling, A., Garg, A., Liu, X., & Peroulis, D. DC-dynamic biasing for >50x switching time improvement in severely underdamped fringing-field electrostatic MEMS actuators. *J. Micromech. Microeng.*22 (2012).
21. Borovic, B., Liu, A. Q., Popa, D., Cai, H., & Lewis, F. L. Open-loop versus closed-loop control of MEMS devices: Choices and issues. *J. Micromech. Microeng.* **15**, 1917-24 (2005).
22. Pons-Nin, J., Rodriquez, A., & Castaner, L. M. Voltage and pull-in time in current drive of electrostatic actuators. *J. Microelectromech. Syst.* **11**, 196-205 (2002).
23. Czaplewski, D. A., *et al.* A Soft Landing Waveform for Actuation of a Single-Pole Single-Throw Ohmic RF MEMS Switch. *J. Microelectromech. Syst.* **15**, 1586-1594 (2006).
24. Elata, D., & Bamberger, H. On the dynamic pull-in of electrostatic actuators with multiple degrees of freedom and multiple voltage sources. *J. Microelectromech. Syst.* **15**, 131-40 (2006).
25. Chen, K.,-S., & Ou, K.-S. Fast positioning and impact minimizing of MEMS devices by suppression motion-induced vibration by command shaping method. *Proc. IEEE 22nd Int. Conf. Micro Electro Mech. Syst. (Sorrento, Italy).* 103-1106 (2009).
26. Chen, K.,-S., Yang, T.,-S., & Yin, J.-F. Residual vibration suppression for duffing nonlinear systems with electromagnetical actuation using nonlinear command shaping techniques. *ASME J. Vibration and Acoustics.* **128**, 778-789 (2006).
27. *Buffered oxide etchant.* MSDS No. B5636 [Online]; Mallinckrodt Baker, Inc.: Phillipsburg, NJ, Septemeber 14, 2009. http://nrf.aux.eng.ufl.edu/_files/msds/299.pdf, accessed March 27 (2013).
28. *Acetone.* MSDS No. A0446 [Online]; Mallinckrodt Baker, Inc.: Phillipsburg, NJ, April 10, 2001. http://www.clean.cise.columbia.edu/msds/acetone.pdf, accessed March 37 (2013).
29. *Isopropyl alcohol.* MSDS No. BDH-140 [Online]; Honeywell: Muskegon, MI, December 29, 2005. http://grice.cofc.edu/pdf/MSDS/Rm205/Plante/Isopropyl%20Alcohol%2099%25.pdf, accessed March 27 (2013).
30. *Hexamethyldisilazane.* MSDS No. H2066 [Online]; Mallinckrodt Baker, Inc.: Phillipsburg, NJ, June 13, 2007. http://kni.caltech.edu/facilities/msds/hmds.pdf, accessed March 27 (2013).

31. *Microposit SC 1827 Positive Photoresist.* [Online]; Rohm and Haas Electronic Materials LLC: Marlborough, MA, April 2, 2004. http://mfc.engr.arizona.edu/safety/MSDS%20FOLDER/Microposit%20SC%201827%20Photoresist.pdf, accessed March 27 (2013).
32. *SUSS MJB 3 mask aligner operator's reference manual rev A.* [Online]; Karl Suss, http://www.acsu.buffalo.edu/~btvu/doc/cr/Suss%20MJB-3%20Operator's%20Manual.pdf, accessed March 27 (2013).
33. *Microposit MF-26A developer.* [Online]; Shipley Europe Ltd.: Coventry, UK, April 7, 2000. http://www.nanotech.wisc.edu/CNT_LABS/MSDS/Developers/MSDS%20MF26A.pdf, accessed March 27, (2013).
34. *Technics 800 Micro RIE Operating Manual.* [Online]; http://research.engineering.ucdavis.edu/cnm2/wp-content/uploads/sites/11/2013/05/Technics800RIE.pdf, accessed July 3, (2014).
35. *Tetramethylammonium hydroxide.* MSDS No. 334901 [Online]; Sigma-Aldrich: Saint Loius, MO, December 12, 2012. http://www.sigmaaldrich.com/MSDS/MSDS/DisplayMSDSPage.do?country=US&language=en&productNumber=334901&brand=SIAL&PageToGoToURL=http%3A%2F%2Fwww.sigmaaldrich.com%2Fcatalog%2Fproduct%2Fsial%2F334901%3Flang%3Den, accessed March 27, (2013).
36. *Hydrofluoric acid.* [Online]; Sciencelab.com, Inc.: Houston, TX, June 9, 2012. http://www.sciencelab.com/msds.php?msdsId=9924296, accessed March 27, (2013).
37. *Piranha clean.* [Online]; Tufts University Standard Operating Procedure: January 12, 2007. http://engineering.tufts.edu/microfab/index_files/SOP/PiranhaClean_SOP.pdf, accessed March 27 (2013).
38. *Transene Sulfite Gold TSG-250.* Product Number: 110-TSG-250; Transene Company: Danvers, MA, January (2012).
39. *Baker PRS-3000™ Positive Resist Stripper.* MSDS No. B0203 [Online]; Mallinckrodt Baker, Inc.: Phillipsburg, NJ, October 31 2001. http://mcf.tamu.edu/docs/msds-pdfs/BAKER-PRS-3000.pdf, accessed March 28 (2013).
40. *Gold etchant type TFA.* Product Number: 060-0015000; Transene Company: Danvers, MA, January (2012).
41. *Xenon Difluoride Etching System.* Lab manual Chapter 7.5 [Online]; Marvell Nanofabrication Laboratory: Berkeley, CA, October 2003. http://nanolab.berkeley.edu/labmanual/chap7/7.5xetch.pdf, accessed March 27 (2013).
42. Garg, A., Small, J., Mahapatro, A., Liu, X., & Peroulis, D. Impact of sacrificial layer type on thin film metal residual stress. *IEEE Sensors (Christchurch, New Zealand).* 1052-1055 (2009).

